SCIENTIFIC REPORTS

OPEN

SUBJECT AREAS:
PERCEPTION
NETWORK MODELS
NEUROPHYSIOLOGY
NETWORK TOPOLOGY

Received
12 April 2013

Accepted
7 August 2013

Published
23 August 2013

Correspondence and requests for materials should be addressed to D.Z.Y. (dyao@uestc.edu.cn)

Cortical network properties revealed by SSVEP in anesthetized rats

Peng Xu[1], ChunYang Tian[1], YangSong Zhang[1], Wei Jing[1], ZhenYu Wang[1], TieJun Liu[1], Jun Hu[1], Yin Tian[1,2], Yang Xia[1] & DeZhong Yao[1]

[1]Key Laboratory for NeuroInformation of Ministry of Education, School of Life Science and Technology, University of Electronic Science and Technology of China, Chengdu, 610054, China, [2]College of Bio-information, ChongQing University of Posts and Telecommunications, ChongQing, China, 400065.

Steady state visual evoked potentials (SSVEP) are assumed to be regulated by multiple brain areas, yet the underlying mechanisms are not well understood. In this study, we utilized multi-channel intracranial recordings together with network analysis to investigate the underlying relationships between SSVEP and brain networks in anesthetized rat. We examined the relationship between SSVEP amplitude and the network topological properties for different stimulation frequencies, the synergetic dynamic changes of the amplitude and topological properties in each rat, the network properties of the control state, and the individual difference of SSVEP network attributes existing among rats. All these aspects consistently indicate that SSVEP response is closely correlated with network properties, the reorganization of the background network plays a crucial role in SSVEP production, and the background network may provide a physiological marker for evaluating the potential of SSVEP generation.

SSVEP can be observed following presentation of a stimulus with a frequency higher than 1 Hz[1,2], where the oscillatory wave responding to the stimuli frequency usually appears in the occipital leads of EEG. However, in practice, only the stimulus with a low frequency, especially in the range below 30 Hz, can effectively evoke a strong SSVEP response characterized by frequency matching of the stimulus or its harmonics. SSVEP is thought to be the physical response of the primary visual cortex to external stimuli[1].

Due to the high signal-to noise (SNR) and relative immunity to artifacts, SSVEP has been widely used in diverse research fields including brain computer interface[3,4], visual attention[5–8], binocular rivalry[9–11] and working memory[12–14]. Using various techniques like EEG, MEG, PET and fMRI, the related studies reveal that the SSVEP response is widely distributed over the occipital and other areas, including parietal, temporal, frontal, and prefrontal areas[15–22]. And these studies implicitly indicate that SSVEPs are the information integration of large-scale brain networks spanning across different cortical areas driven by flickering. Meanwhile, the pre-state EEG background has a large influence on cognitive processes[5,13], thus SSVEP responses may also be related to this baseline state.

In recent years, brain network theory has shown increasing application in neuroscience. Using correlation analysis of fMRI data collected during a stable state visual stimulus, Srinivasan showed that occipital voxels were positively or negatively correlated to the frontal voxels forming functionally distinct large-scale functional networks, and the response of the medial frontal cortex depended on the stimulation frequencies[18]. Using the directed transfer function, Yan et al. constructed the effective connectivity pattern of SSVEP based on the scalp EEG, and showed that the parietal regions were a critical node for SSVEP information transmission[23]. Due to the involvement of multi-brain areas during SSVEP generation, network analysis may be a potential tool for the study of SSVEP neural mechanism, which may provide the new insights for SSVEP from network aspect.

Though various techniques have been adopted for SSVEP related studies, the SSVEP neural mechanism are still not well understood, especially the brain network associated with SSVEP are less reported, such as what is the network difference between a low frequency stimuli that can evoke strong SSVEP and a high frequency stimuli that cannot have strong SSVEP, which network properties are correlated with the strength of SSVEP, and is there relationship between the background neural activities and SSVEP? The reliable recording technique and suitable analysis are crucial to reveal those concerned aspects. The usual recording techniques for SSVEP studies can be divided into electrophysiology and metabolism. Those electrophysiological recordings like scalp EEG has such drawbacks as coarse position information and volume conductivity effect, while the metabolism ones including fMRI and PET cannot record the dynamic SSVEP response well due to their intrinsic low temporal resolution. In

the present study, the multi-channel intracranial recordings are used to investigate the network of SSVEP based on rat. Compared to the existing studies, the utilization of multi-channel intracranial EEG recordings and network analysis may have below advantages for SSVEP neural mechanism study: 1) The multi-channel intracranial EEG recordings may provide both reliable dynamic waveform and precise cortex positions; 2) The network analysis can probe interactions among specific brain areas, which may be of more potential to reveal the underlying neural mechanism of SSVEP.

Results

SSVEP response difference for different frequency stimuli. Figure 1(a) shows the original intracranial EEG waveform on electrode V1_L of one rat for 8 Hz, 44Hz and 84 Hz stimuli, respectively. Based on the FFT transformation for the 2 minute long recordings, the averaged SSVEP responses on the 12 electrodes over 10 rats for the three frequency stimuli are given in Figure 1(b)∼(d), where the strong SSVEP response of 8 Hz can be consistently observed on all the 12 electrodes, and only very weak response can be observed on some sites like V1, V2 and PtA for 44 Hz and 84 Hz stimuli. This finding also demonstrates that SSVEP can be evoked under anesthesia.

In the following analyses, the related SSVEP strengths are calculated from the corresponding EEGs at electrode V1_L based on the reliable 8 Hz responses observed on electrode V1_L with the smallest STD revealed in Figure 1.

Cortical networks activated by flickers of different frequencies. Based on the selected 3s-long EEG, the averaged network properties across 10 rats for the four conditions are shown in Figure 2 by varying the network binarization thresholds. Figure 2 demonstrates that the network corresponding to 8 Hz stimulus exhibit larger clustering coefficients (C), higher local efficiency (Le) and global efficiency (Ge), and shorter characteristic path length (L) compared to the networks at 44 Hz and 84 Hz stimuli. Further, the network properties of the 44 Hz and 84 Hz stimuli did not have obvious difference compared to that of control state network, while the 8 Hz stimulus showed a large difference in network properties from the control state. The paired t test reveal that, the four network properties of the 8 Hz stimulus were significantly different from those corresponding to the 44 Hz, 84 Hz, and control states for most of the tested thresholds.

The topology differences between the three stimuli frequencies and the control state across 10 rats are shown in Figure 3(a), where the paired t test is performed to investigate the linkage difference for each edge. The network topology changes shown in Figure 3(a) demonstrate that the network corresponding to the 8 Hz stimulus had a very strong increase in linkage strength between the frontal area and the parietal lobe compared to the control state network, while the 44 Hz and 84 Hz networks had no obvious difference compared to the control state. The differences in network topologies among the three stimuli conditions are further shown in Figure 3(b), where the 8 Hz network also exhibits a more dense linkage between the frontal

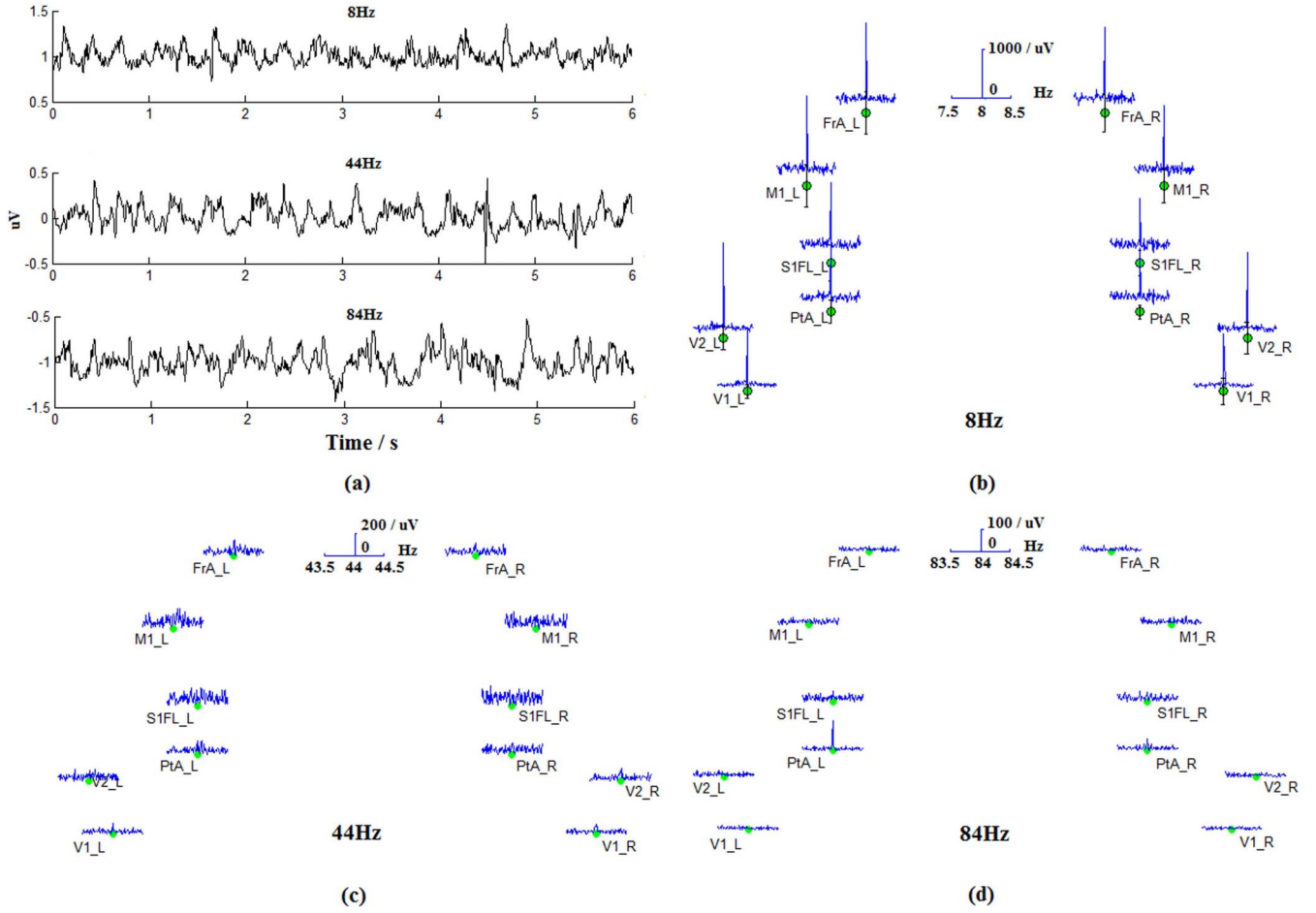

Figure 1 | The SSVEP responses for the three frequency stimuli on 12 electrodes averaged over 10 rats. (a) The original intracranial EEG waveforms of one rat at electrode V1_L for the three stimuli; (b) 8 Hz spectrum in range 7.5 Hz ∼ 8.5 Hz; (c) 44 Hz spectrum in range 43.5 Hz ∼ 44.5 Hz; (d) 84 Hz spectrum in range 83.5 Hz ∼ 84.5 Hz. In (b) ∼ (d), blue curve indicates the SSVEP response and green dot represents the position of electrode. In (b), the black vertical line denotes the standard deviation (STD) of 8 Hz response for 10 rats on each electrode.

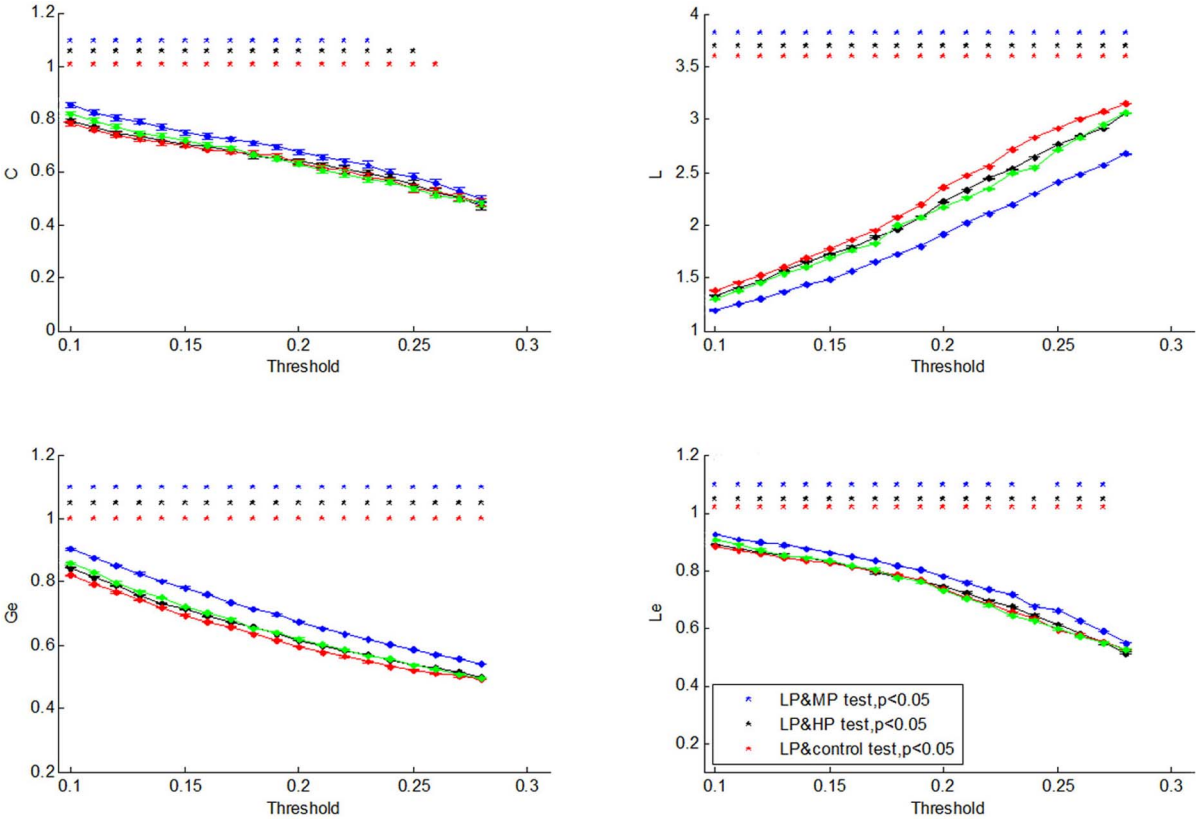

Figure 2 | The network properties varied with different network thresholds. The green line represents the control state, blue line represents the 8 Hz stimulus, black line represents the 44 Hz stimulus, and the red line represents the 84 Hz stimulus. The blue * indicates a significant difference ($p<0.05$) between the 8 Hz and 44 Hz stimulus networks. The black * indicates a significant difference ($p<0.05$) between 8 Hz network and 84 Hz network. The red * indicates a significant difference ($p<0.05$) between the 8 Hz stimulus and control state networks ($p<0.05$).

and occipital areas, and between the parietal and occipital lobes, compared to the other two stimuli conditions. The hub coefficients shown in Figures 3(a) and (b) show that the parietal lobe plays an important role in SSVEP generation, which is consistent with previous results using scalp EEG[23]. The relatively shorter *L*, larger *Ge*, *Le* and *C* indicate that the network corresponding to the 8 Hz stimulus has more effective information processing ability in both local and global regions. We assume this might be the main reason why 8 Hz stimulus can evoke the strong SSVEP while the other two frequencies cannot.

Dynamic SSVEP Strength versus Dynamic Network Organization in Individual Rat. Based on the observation that the SSVEP strengths of each individual rat were varied during the experiment, we hypothesized that the corresponding network properties and SSVEP for each rat may have a dynamic relationship. Using the network properties and SSVEP strengths calculated from the segments selected from individual rat, the dynamic relationship between 8 Hz-SSVEP strength and network properties was calculated under various thresholds for each rat. Figure 4(a) visually shows the relationship between network properties and SSVEP strength under 0.28 threshold for one rat, and other threshold also shows the similar relationship.

As shown in Figure 4(a), *C*, *Ge* and *Le* exhibited a strong positive correlation with SSVEP strength, and *L* behaved negatively correlated to SSVEP strength. The averaged relationships across thresholds 0.10 ~ 0.28 for each rat are given in Table 1, which shows the similar relationships for all the 10 rats. Figure 4(b) specifically compared the network topologies corresponding to the states having largest and smallest SSVEP responses with that of control state for the corresponding rat in Figure 4(a), where the network topology of largest SSVEP response has much denser linkages. All these facts inferred that reorganization of the network towards enhanced efficiency by external stimulus would benefit the generation of SSVEP.

SSVEP Strength versus Network Organization in Group Level. In the experiment, though all the rats are fostered at the same time, they still have a quite different SSVEP strength. For each threshold, the topological properties and SSVEP strengths under the 8 Hz stimulus state are averaged over all segments selected for each rat. The detailed relationships between 8 Hz network properties and 8 Hz SSVEP strengths among group rats for the various thresholds (0.10 ~ 0.28) are given in below Figure 5(a), where the strong correlations between the 8 Hz-SSVEP strength and the four network properties are observed, with negative correlations for *C*, *Ge* and *Le*, and a positive correlation for *L*.

Figure 6(a) visually shows the corresponding relationship between 8 Hz network properties and 8 Hz SSVEP strengths for the group rats under 0.28 threshold. Those relationships revealed in Figure 5(a) and Figure 6(a) are contrary to those obtained from the individual rat as shown in Figure 4(a).

Figure 5(b) gives the corresponding relationships between control network properties and 8 Hz SSVEP strengths among group rats for the various thresholds (0.10 ~ 0.28). Figure 6(b) visually shows the corresponding relationship between control network properties and 8 Hz SSVEP strengths for the group rats under 0.28 threshold. Figure 6(c) further shows the network topology of rat 5 and 10, which have the smallest and largest SSVEP responses, respectively. As shown in Figure 6(c), rat 5 has a more efficient background network and stimulus network than rat 10. Both Figure 5 and Figure 6 reveal similar relationships for SSVEP strengths and network properties.

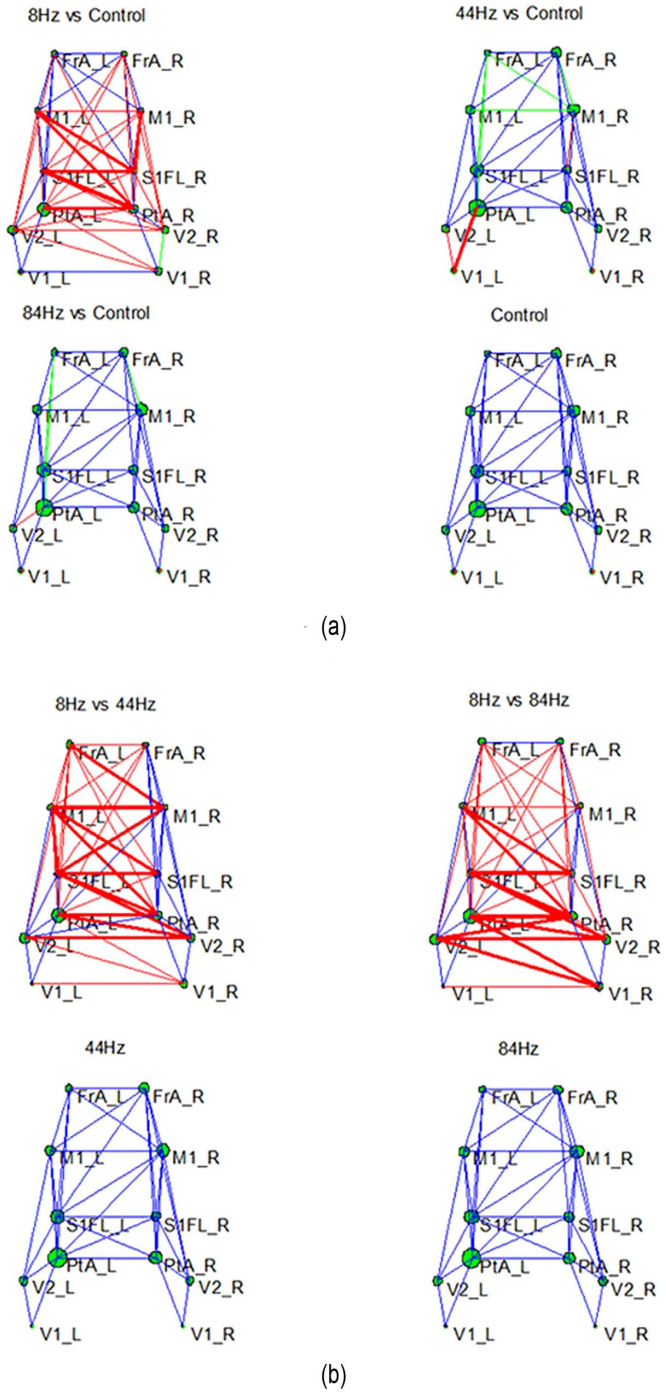

Figure 3 | The network topology for the four conditions. (a) The network topology difference between the three frequency stimuli networks and the control state network. The actual anatomic coordinates of these nodes are illustrated in Figure 7; (b) The network topology difference between the 8 Hz network and the other two frequency stimuli networks. Based on two paired *t*-tests, the red line denotes the edges with a statistically significant increase ($p<0.05$) in linkage between the compared two networks, and the thickness of the edge indicates the strength of the increase. The green line denotes a significant decrease ($p<0.05$) in strength, while the blue lines denote no statistical difference between the two compared networks. The size of green circle represents the Hub coefficients of each node.

Tables 2∼5 shows the close correlations of the network properties between the 8 Hz-network and control network for various threshold (0.10 ∼ 0.28). All these relationships in Figure 5∼6 and Table 2∼5 suggest that the baseline network may have played an important role in SSVEP generation, and the contrary relationships between Figures 4(a) and Figure 6(a) might be due to the effect of the background activities.

Discussion

Similar to the SSVEP responses reported in previous studies, the low 8 Hz stimulus evoked a very strong SSVEP response with very high signal-to-noise-rate (SNR) on all 12 electrodes, while only some weak responses on electrodes like V1, V2 and PtA can be observed for 44 Hz and 84 Hz stimuli. This phenomenon demonstrates that relatively higher frequency stimuli are not suitable for SSVEP application like BCI due to the relatively lower SNR response. The appearance of 8 Hz SSVEP response on 12 electrodes prove that SSVEP generation is involved with multi-brain areas including both the visual related areas and the non-visual cortex like frontal association cortex, primary motor cortex and primary somatosensory cortex, etc. Therefore, it is more meaningful to study the SSVEP neural mechanism by considering the interactions among those related brain areas. The observation of the 8 Hz SSVEP response under anesthesia also provides proof that SSVEP is the physical response to the external stimuli.

Figure 2 demonstrates that whatever binarized thresholds of network were adopted, the networks responding to the 8 Hz stimulus consistently exhibit a larger *C* and a higher *Le* and *Ge*, as well as a shorter *L* compared to those corresponding networks of 44 Hz, 84 Hz, and controls. The four network properties can be divided into two aspects, one consisting of *C* and *Le* denoting the local information processing abilities of networks, and the other consisting of *L* and *Ge*, representing the processing and transfer abilities of global information in the network. The difference in the network properties and topology in Figures 2 and 3 demonstrates that SSVEP is highly related to a network consisting of multiple brain areas, and 8 Hz network was more efficient in both local and global information processing than the other two stimuli. As SSVEP response can be regarded as the signal enhancement or transfer of the external stimuli in brain, it is reasonable to assume that if a stimulus can evoke the corresponding SSVEP response, the corresponding response network should have powerful processing and stable transferring ability to keep the information of the flickering stimuli intact as possible. The network organization in Figure 3 demonstrates that the 8 Hz networks have much more efficient connection between the frontal area and the posterior parietal lobe, and also between the posterior parietal lobe and the occipital lobe, than the networks of the other two stimuli. The mentioned network topology difference may guarantee an intact and efficient information processing and transfer for 8 Hz SSVEP stimulus, resulting in a relatively stronger SSVEP response. The Hub nodes in the 8 Hz network indicated that the parietal lobe had the largest hub coefficient, suggesting that the parietal lobe plays an important role in the generation of SSVEP, which is consistent with previous report using scalp EEG in humans[23].

The scatter plot in Figure 4(a) demonstrates that the SSVEP response also varied across time for each rat during experiment. Table 1 consistently indicate a strong synergetic dynamic relationship between SSVEP strength and the four network properties across the various network thresholds (0.10 ∼ 0.28) for all rats. Specifically, both *C* and *Le* were positively correlated with SSVEP strength, suggesting that the efficient processing of local information favors a strong SSVEP generation. Meanwhile, the negative relationship between SSVEP and *L* and the positive relationship between SSVEP and *Ge* confirm that the efficient global information processing ability also benefits SSVEP generation.

Furthermore, the network topologies corresponding to the smallest and largest SSVEP responses of a rat shown in Figure 4(b) reveal that, when the largest SSVEP response occurs, the network will have more increased linkages from control network than the network

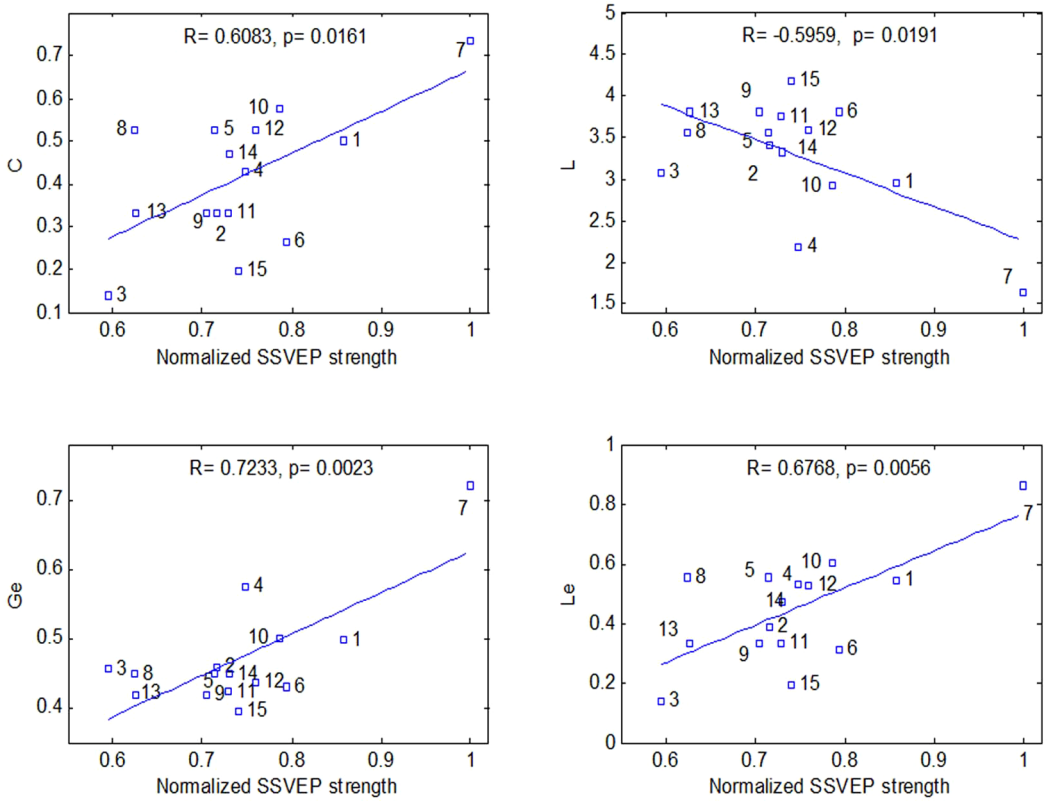

(a)

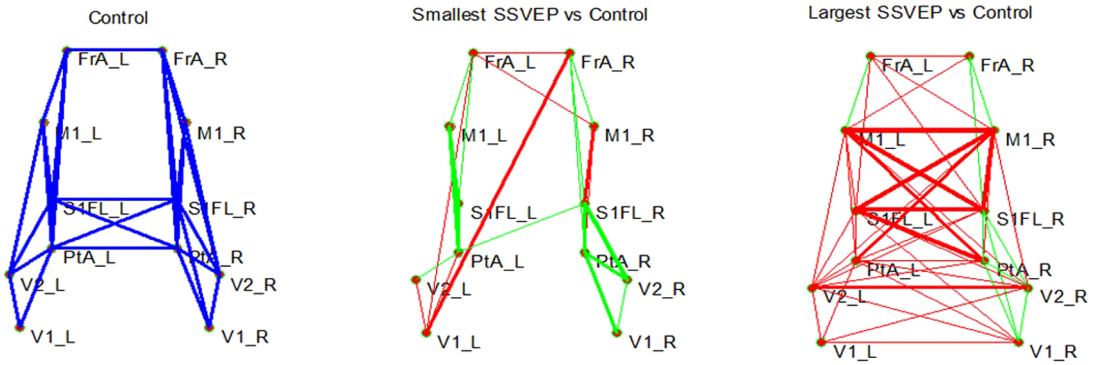

(b)

Figure 4 | The dynamic changes of the SSVEP strength and the four network properties for one rat under 0.28 threshold. (a) The correlation between SSVEP strength and the network properties. The x-axis indicates the 8 Hz SSVEP strength normalized by the largest SSVEP strength of the same rat. The number close to the square dots represents the 3s-long segment index. *R* indicates the correlation coefficients, and *p* represents the statistical values for the relationship. (b) The network organization for the largest and smallest SSVEP responses compared to the control state for this rat. The red line denotes the edges that have increased linkage between the compared two networks, and the thickness of the edge delineates the increased strength. The green lines denote the decreased linkage edge with thickness delineating the decreased strength.

corresponding to the lowest SSVEP response. These results suggest that the dynamic variation of the network reorganization over time likely results in the dynamic variation of SSVEP responses for individual rats, i.e., the higher the efficiency of the network at a moment, the larger the SSVEP strength is.

Figure 6(b) shows that the SSVEP strength is closely correlated with the network properties of the control state under the largest 0.28 threshold, and the consistent relationships also exist for other thresholds (0.10 ~ 0.28) as shown in Figure 5(b). As the network at the control state mainly reflects the baseline activation, a more efficient network may indicate the more robustness to the external stimulus, i.e., the more efficient and stable the network at baseline, the more difficult to disrupt with an external stimulus. As for our 8 Hz stimulus in the experiment, the strength was maintained relatively constant across the different rats due to the relatively fixed position of the LED and the consistent voltage used to drive the LED, thus the rats with lower network efficiency at baseline instead exhibited greater responses to the stimuli because of its relative lower activated threshold for external stimulus (Figure 5(b) and Figure 6(b)).

Comparing the relationships in Figure 6(a) and Figure 4(a), the concerned trends evaluated at group level (Figure 6(a)) is contrary to that revealed on the individual rat (Figure 4(a)), and this contrary relationship can also be observed in Table 1 and Figure 5(a) for the various thresholds (0.10 ~ 0.28). What leads to the contrary

Table 1 | The relationships between SSVEP strength and the four network properties for each rat

	C	*L*	*Ge*	*Le*
RAT1	0.419 ± 0.069	−0.631 ± 0.015	0.664 ± 0.013	0.521 ± 0.054
RAT2	0.099 ± 0.099	−0.428 ± 0.026	0.441 ± 0.029	0.253 ± 0.080
RAT3	0.604 ± 0.029	−0.613 ± 0.019	0.610 ± 0.015	0.640 ± 0.029
RAT4	0.439 ± 0.068	−0.535 ± 0.026	0.539 ± 0.027	0.476 ± 0.070
RAT5	0.562 ± 0.037	−0.528 ± 0.037	0.535 ± 0.035	0.562 ± 0.036
RAT6	0.461 ± 0.048	−0.690 ± 0.013	0.729 ± 0.008	0.545 ± 0.038
RAT7	0.673 ± 0.031	−0.678 ± 0.027	0.717 ± 0.024	0.692 ± 0.027
RAT8	0.606 ± 0.034	−0.716 ± 0.013	0.806 ± 0.019	0.593 ± 0.026
RAT9	0.559 ± 0.030	−0.629 ± 0.014	0.720 ± 0.016	0.566 ± 0.025
RAT10	0.446 ± 0.032	−0.561 ± 0.021	0.580 ± 0.020	0.432 ± 0.032

For each rat, the value is averaged across threshold 0.10 ~ 0.28 with step 0.01.

relationships between group and individual levels? We propose that when the relationships are evaluated among rats, the different baseline conditions of the individual rat may have a strong effect on the relationship among rats. And this assumption is further supported by the strong positive coupling between the network properties of the background control state and the 8 Hz stimulus state shown in Tables 2~5. Based on the large correlation coefficient in Tables 2~5 and the similar relationships in Figures 5(a) and 5(b), and in Figure 6(a) and 6(b), the contrary trends in Figures 6(a) and 4(a) may reflect the role of the intrinsic background network to the stimulus state. The proportional ratio k smaller than 1.0 in Tables 2~5 also demonstrates that rats with less efficient background processing networks will instead show relatively greater network disturbances in response to a similar stimulus. In our experiment, rats 5 and 10 exhibited the smallest and largest SSVEP responses, respectively. Figure 6(c) further revealed the networks of the control states for those two rats were markedly different, with rat 5 exhibiting a more efficiently linked background network than rat 10. Therefore, due to the higher efficiency level of the intrinsic background network existing in rat 5, rat 10 exhibited a much stronger SSVEP response instead (i.e., rat 10 has a greater potential to be disturbed by the external frequency stimulus).

Figure 5, Tables 1~5 demonstrates that the thresholds used to binarize the network actually have influence on the concerned relationships between SSVEP strength and network properties. But the consistent relationships can be found for most thresholds with correlation coefficients larger than 0.4, which can prove that those established relationships are robust across different thresholds.

The above results indicated that an inefficient default network would facilitate SSVEP. Reference to the fMRI study of default mode network (DMN) regarded as a task-negative network, the negative correlation of SSVEP strength with the baseline network efficiency may account for the similar physiological basis.

The aim of our study was to examine the possible relationships between SSVEP generation and brain networks. We used anesthetized animals to exclude the potential effects of other high-level cognition processes, to lower the unexpected artifacts induced by body movement, and to provide a more consistently stable stimulus during the experiment. Awake rats will reflexively close their eyes or move their heads to avoid the flicker stimulus. As SSVEP is the fundamental physical response of external frequency stimuli, our results confirmed that SSVEP information still can be observed under anesthesia, as reported in the previous study[24]. However, it is possible that there are differences in the SSVEP recorded between the normal (awake) and anesthetized states, as there is some evidence showing that higher level cognition activity may be partially involved in SSVEP[12]. The existing study has revealed that the topological network features can be well maintained even in the anesthetized brain[24]. Therefore, it is likely to assume that the similar reorganization of brain network may be observed between normal and anesthesia states. However, future studies on the awaken state are required to confirm this assumption.

In the present study, we used multi-channel intracranial EEG recordings and network analysis to study the neural mechanism of SSVEP in rats, and it provides the following new aspects to infer the relationship between SSVEP generation and brain networks: 1) Due to the results that the evoked brain network corresponding to 8 Hz stimulus is of much denser linkage, and of much information processing ability compared to the networks of the other two stimuli without obvious SSVEP observed, we assume that this network difference may be correlated with the SSVEP difference among different frequency stimuli; 2) As the dynamic fluctuation of SSVEP for individual rats is correlated with the properties of the response network, and a stronger SSVEP response has a more efficient brain network, we argue that SSVEP generation is related with the brain network reorganization; 3) Owing to the more efficient and stable the network is at baseline, the weaker is the SSVEP strength, we infer that an originally efficient network is hard to be reorganized to induce a response by an external stimulus, and so the network properties of the baseline may serve as a potential biomarker for the prediction of SSVEP response, i.e., rats with less efficient local or global information processing ability at baseline may have a relatively strong SSVEP response.

Currently, the view of SSVEP generation is still controversial. Some researchers use the traveling waves to explain the SSVEP generation[1,25], and other related studies assume that SSVEP is generated by the specific source at special location such as occipital or parietal, as well as by the sources widely distributed over brains[2]. Based on the above results, we assume that generation of SSVEP is closely correlated with the reorganization of brain networks with nodes distributed in the whole brain. This result may naturally encourage a network orienting integration route in SSVEP based cognitive neuroscience study of the brain in the future.

However, we must admit that human brain is much different from that of rat in both structure and function, and those findings in rats may not be directly inferred to human. In future, we will perform simultaneous EEG and fMRI on humans to further reveal the possible difference of SSVEP mechanism existed between human and rat. Moreover, though the current experiment and analysis show a close relationship between SSVEP response and network properties, and it may infer the network reorganization plays an important role for SSVEP generation. But we must admit that the current work cannot provide a definite conclusion that whether network change is the causality accounting for the SSVEP generation or just the consequence of the external stimuli, the reach of which needs other causal experiment.

Methods

All experiments were approved by the Ethical Committee on Animal Experimentation of University of Electronic Science and Technology of China (UESTC).

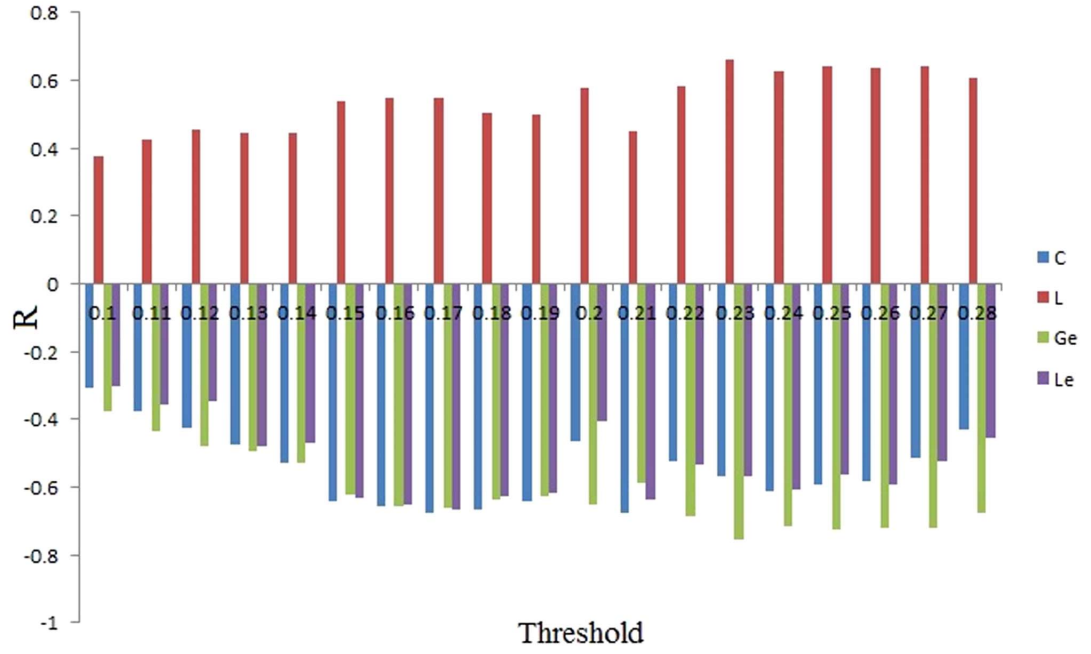

(a)

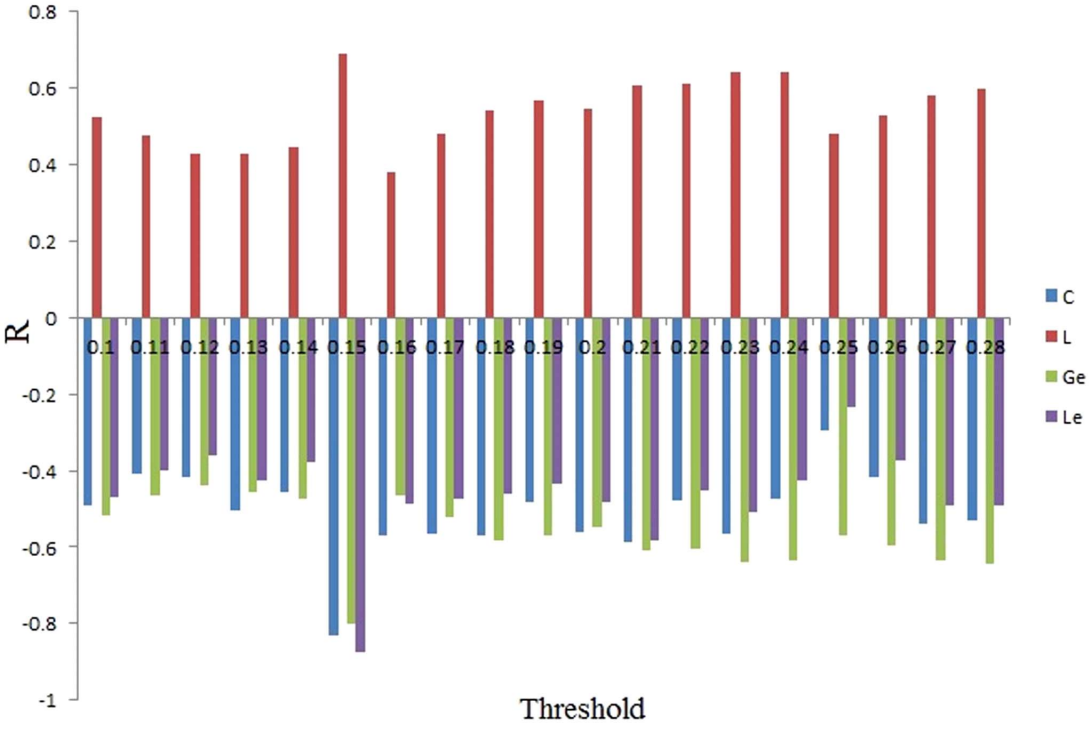

(b)

Figure 5 | The relationships of SSVEP strength and network properties at group level for various thresholds (0.10 ~ 0.28). (a) SSVEP strength versus 8 Hz stimulus network properties; (b) SSVEP strength versus control network properties. In (a) ~ (b), the x-axis is the threshold, and y-axis is the corresponding correlation coefficients for the four network properties.

Rats and EEG recording. Ten male Wistar rats (body weight 290–320 g) were included in the study. Electrode implantation was performed under general anesthesia (sodium pentobarbital 60 mg/kg bodyweight, i.p.), complemented with 0.6 ml atropine sulfate (0.5 mg/ml, s.c.) to prevent excessive secretion. During stereotactic surgery, wounds were infiltrated with lignocaine (2%). Additional pentobarbital (15 mg/kg) was given intraperitoneally when required. All stereotactic coordinates were relative to bregma with the skull surface flat, according to Paxinos and Watson (2005)[26]. Thirteen small holes were drilled in the skull over the frontal area, primary motor area, primary somatosensory cortex, parietal lobe, and primary (secondary) visual cortex (regions potentially involved in SSVEP generation), and the temporal muscle was incised and drilled vertically to skull surface flat. Stainless-steel screw electrodes (diameter, 200 μm) were implanted in the drill holes, with the reference set at cerebrum (Cb), which exhibits lower activity compared to other brain sites[27,28]. The 13-electrode montage is shown in Figure 7.

After surgery, animals were recovered for one week in individual cages with a 12 : 12 h light: dark cycle (lights on at 8:00 A.M daily). After one week recovery period, the SSVEP experiment was carried out. During the experiments, the head of each rat was fixed using a specially designed box with a small hole through which the

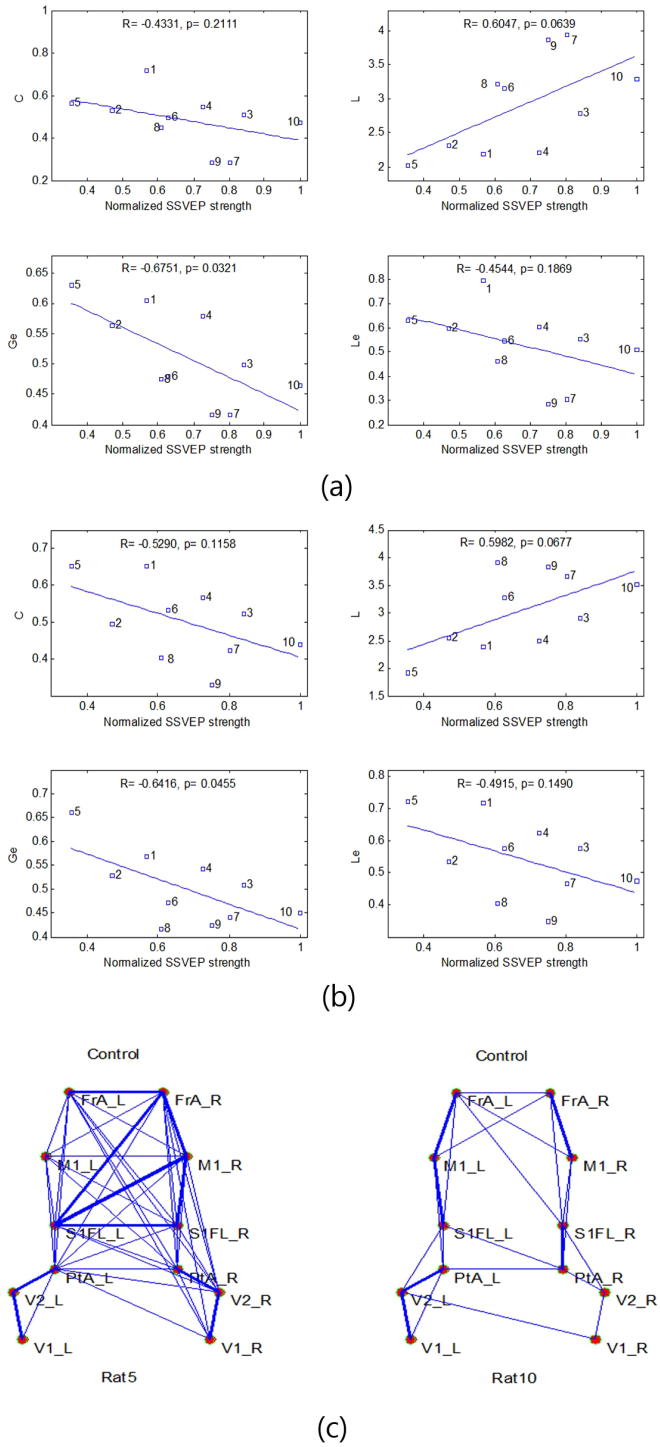

Figure 6 | SSVEP strength versus network properties at group level under 0.28 threshold. (a) The 8 Hz SSVEP strength versus network properties of the stimulus state. (b) The 8 Hz SSVEP strength versus the network properties of the control state. (c) The control network topologies of rat 5 with smallest SSVEP strength and rat 10 with largest SSVEP strength. In (a) ~ (b), the number close to the square dots indicates the rat index, and the SSVEP strength normalization is based on the maximal SSVEP response of the 10 rats, *R* indicates the correlation coefficients, and *p* represents the statistical values for the relationship.

head can protrude but not move freely. Rats were injected with sodium pentobarbital (60 mg/kg body weight) for general anesthesia to further reduce unexpected artifacts induced by body movement, to exclude the effect of other higher level cognitive activity, and to provide a more stable stimulus during the whole experiment. SSVEP has been shown to be able to be evoked under such anesthesia state[29].

Table 2 | The coupling relationship between clustering coefficients of 8 Hz network and control network

C		y = ax + b*	
Threshold	R	a	b
0.10	0.785	0.64	0.31
0.11	0.745	0.88	0.06
0.12	0.805	0.86	0.09
0.13	0.893	0.85	0.10
0.14	0.867	0.82	0.11
0.15	0.831	0.70	0.21
0.16	0.903	0.82	0.10
0.17	0.767	0.63	0.21
0.18	0.804	0.66	0.21
0.19	0.635	0.57	0.25
0.20	0.744	0.67	0.20
0.21	0.903	0.99	−0.01
0.22	0.867	0.78	0.12
0.23	0.815	0.95	0.03
0.24	0.814	1.07	−0.04
0.25	0.736	0.91	0.05
0.26	0.871	0.90	0.05
0.27	0.860	1.11	−0.11
0.28	0.865	1.04	−0.04
Mean	0.816 ± 0.069	0.83 ± 0.16	0.10 ± 0.11

*The linear form ($y = kx + b$) is used to model the relationship between the two states with control being variables *x*. *R* is the correlation coefficients between the network properties at stimulus and control states.

Experiments were carried out in a room with thick black curtain to shade the natural light. Before the frequency stimulus, a 5 min control period was recorded for each rat. Next, rats were sequentially exposed to the 8 Hz low frequency stimulus, the 44 Hz middle frequency stimulus, and the 84 Hz high frequency stimulus provided by a LED with tunable frequencies. The duration time for each stimuli frequency was 2 min, and 2 min rest was adopted before each frequency stimulus. The LED was fixed approximately 6 cm over the nose of the rat, with a 7 voltage fed to the LED for all the stimuli. EEG was recorded with a UEA-FZ amplifier (SYMPTO Company, BeiJing, China) using compatible software developed by our lab (1000 Hz sampling rate), and was filtered using a 50 Hz notch filter and band pass filter 0.1–120 Hz. All recordings were stored on a hard disk (Lenovo Company, NewYork, USA) for further analysis.

Table 3 | The coupling relationship between characteristic path length of 8 Hz network and control network

L		y = ax + b	
Threshold	R	a	b
0.10	0.787	0.50	0.59
0.11	0.698	0.52	0.62
0.12	0.778	0.61	0.50
0.13	0.847	0.66	0.45
0.14	0.820	0.65	0.51
0.15	0.918	0.70	0.41
0.16	0.865	0.84	0.25
0.17	0.858	0.86	0.25
0.18	0.671	0.49	0.93
0.19	0.647	0.46	1.03
0.20	0.679	0.55	0.91
0.21	0.769	0.67	0.65
0.22	0.829	0.68	0.70
0.23	0.886	0.97	0.16
0.24	0.942	0.96	0.12
0.25	0.829	0.74	0.63
0.26	0.896	0.74	0.61
0.27	0.882	0.88	0.23
0.28	0.929	0.94	0.04
Mean	0.817 ± 0.090	0.71 ± 0.16	0.50 ± 0.28

Table 4 | The coupling relationship between global efficiency of 8 Hz network and control network

Ge		y = ax + b	
Threshold	R	a	b
0.10	0.791	0.52	0.44
0.11	0.700	0.55	0.38
0.12	0.781	0.64	0.30
0.13	0.841	0.67	0.26
0.14	0.815	0.65	0.26
0.15	0.910	0.70	0.25
0.16	0.852	0.81	0.13
0.17	0.869	0.89	0.08
0.18	0.741	0.61	0.26
0.19	0.719	0.57	0.28
0.20	0.764	0.67	0.20
0.21	0.794	0.72	0.18
0.22	0.867	0.76	0.14
0.23	0.915	0.91	0.03
0.24	0.942	0.90	0.05
0.25	0.892	0.79	0.11
0.26	0.924	0.80	0.11
0.27	0.900	0.89	0.06
0.28	0.926	0.93	0.05
Mean	0.839 ± 0.075	0.74 ± 0.13	0.19 ± 0.12

Coherence. Coherence represents the linear relationship at a specific frequency between two signals $x(t)$ and $y(t)$[30], which can be expressed as[31],

$$Coh_{xy}(f) = \frac{|S_{xy}(f)|^2}{S_{xx}(f)S_{yy}(f)} \quad (1)$$

where $S_{xy}(f)$ is the cross-spectrum between $x(t)$ and $y(t)$, while $S_{xx}(f)$ and $S_{yy}(f)$ are the auto-spectra calculated from a Fast Fourier Transform (FFT) performed on $x(t)$ and $y(t)$, respectively.

Network analysis. Network analysis was performed using the 12-electrodes as the nodes. The coherence between electrode pairs was used to measure the interactions between two regions. The averaged coherence in the 4 Hz ~ 98 Hz range between each node pair was treated as the linking strength of the network. After the weighted network was calculated, a threshold that can guarantee the connection of network was used to binarize the network. Based on the binarized network, the local and global characteristics of the network can be quantitatively denoted by the network measurements including clustering coefficient (C), characteristic path length (L), local efficiency (Le), and global efficiency (Ge)[32].

Let W be the weighted adjacent matrix with w_{ij} denoting the connection between node i and j, N be the node number and Ω be the set of all nodes in the network. For a given threshold T, the adjacent matrix W is binarized as,

$$w_{ij} = \begin{cases} 1, & w_{ij} \geq T \\ 0, & w_{ij} < T \end{cases} \quad (2)$$

The degree denoting the number of links connected to node i is defined as,

$$k_i = \sum_{j \in \Omega} w_{ij} \quad (3)$$

The number of triangles associated with node i is,

$$t_i = \sum_{j,h \in \Omega} w_{ij} w_{ih} w_{jh} \quad (4)$$

Let d_{ij} represent the shortest path length between node i and node j, the corresponding characteristics path length is,

$$L = \frac{1}{N}\sum_{i \in \Omega} L_i = \frac{1}{N}\sum_{i \in \Omega} \frac{\sum_{j \in \Omega, j \neq i} d_{ij}}{N-1} \quad (5)$$

The clustering coefficient can be calculated as,

$$C = \frac{1}{N}\sum_{i \in \Omega} \frac{2t_i}{k_i(k_i-1)} \quad (6)$$

Based on the shortest path length d_{ij} between node i and node j, global efficiency is defined as,

$$E_{global} = \frac{1}{N}\sum_{i \in \Omega} \frac{\sum_{j \in \Omega, j \neq i} d_{ij}^{-1}}{N-1} \quad (7)$$

And the local efficiency is,

$$E_{loc} = \frac{1}{N}\sum_{i \in \Omega} \frac{\sum_{j,h \in \Omega, j \neq i} w_{ij} w_{ih} [d_{jh}(\Omega_i)]^{-1}}{k_i(k_i-1)} \quad (8)$$

Table 5 | The coupling relationship between local efficiency of 8 Hz network and control network

Le		y = ax + b	
Threshold	R	a	b
0.10	0.807	0.62	0.35
0.11	0.770	0.95	0.02
0.12	0.860	0.94	0.04
0.13	0.923	0.84	0.13
0.14	0.835	0.91	0.07
0.15	0.806	0.71	0.24
0.16	0.915	0.87	0.08
0.17	0.810	0.82	0.12
0.18	0.787	0.76	0.16
0.19	0.680	0.64	0.26
0.20	0.727	0.62	0.27
0.21	0.876	1.04	−0.04
0.22	0.871	0.82	0.11
0.23	0.803	0.94	0.04
0.24	0.791	1.11	−0.08
0.25	0.717	0.86	0.09
0.26	0.837	0.85	0.09
0.27	0.840	1.12	−0.08
0.28	0.864	1.05	−0.04
Mean	0.817 ± 0.064	0.87 ± 0.15	0.10 ± 0.12

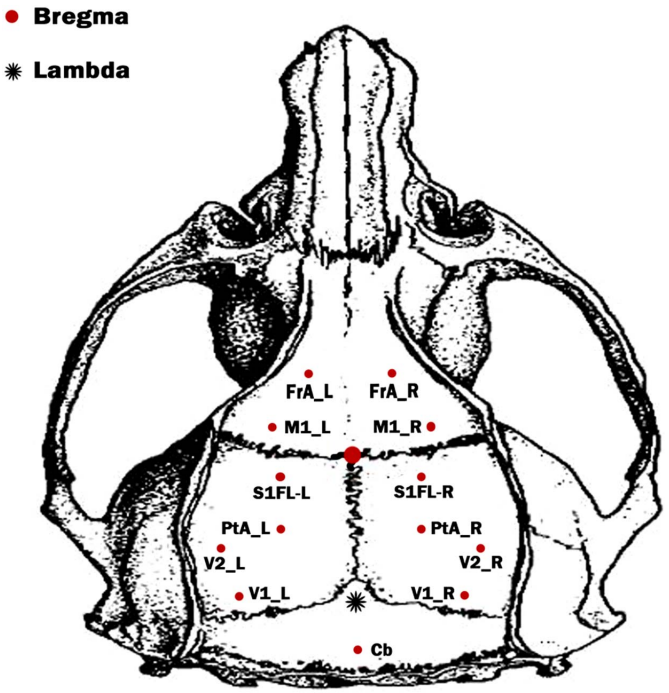

Figure 7 | The distribution of the intracranial electrodes. Detail of those positions are: L, left;_R, right; FrA, frontal association cortex; M1, primary motor cortex; S1FL, primary somatosensory cortex, forelimb region; PtA, parietal association cortex; V2, secondary visual cortex; V1, primary visual cortex; Cb, cerebellum. This figure was produced by Wei Jin and Jun Hu.

where $d_{jh}(\Omega_i)$ is the shortest path length between node j and node h that only contains neighbors of i.

In the following analysis, based on the weighted network matrix of each rat, the differential network topology between two concerned conditions is calculated by the subtraction of corresponding weighted network matrix. After the subtraction of weighted network matrix, the paired t test is further performed to evaluate whether the edge difference is of statistical sense ($p<0.05$) in the differential networks across rats (See the differential topologies in Figure 3(a)∼(b)).

Data Processing. Based on the network analysis and FFT transformation, we examined different relationships between SSVEP generation and brain network following below analysis.

1)SSVEP response recognition. To reveal the SSVEP response, the 2 minutes long recordings for the 3 stimuli are directly applied to FFT transformation for each electrode. And the peak amplitude at stimulus frequency in the spectral domain was treated as the corresponding strength of the SSVEP response.

2)Cortical networks activated by flickers of different frequencies. The 2 minutes long recordings for each stimulus condition were further divided into small non-overlapping 3s long segments. The segments free of EMG and motion artifacts were selected for further analysis. Due to the different duration of artifacts in the 10 rats, the number of 3s-long segments are varied across 10 rats and the three stimuli conditions within range 10 ∼ 16 segments. Similarly, 10 non-overlapping 3s long segments free of artifacts are selected from the 5 minutes long recordings of control state for each rat.

Network analysis is performed to each segment for various thresholds between 0.10 and 0.28. The selection of this threshold range is based on two criteria, one is that the network cannot be too densely connected resulting in the regular networks (>0.10), another is that network should be fully connected without any isolated node (<0.28). For each rat, the corresponding network properties are averaged across selected segments to estimate the individual network properties under different stimulus conditions and control state for each threshold. Then the individual network properties are further averaged across 10 rats for each condition. By varying the network thresholds from 0.05 to 0.28 with 0.01 step, the network parameters versus the network threshold curves were estimated. For each threshold, a paired t test was performed to investigate the differences between the network measurements of the four conditions across 10 rats.

3)Dynamic evolution of SSVEP versus network properties in individual rats. The above FFT transformation reveals that 8 Hz stimulus can evoke an obvious SSVEP compared to 44 Hz and 84 Hz stimuli. However, SSVEP response will be varied during the experiment even for one rat. To reveal the possible dynamic relationships during experiment, the FFT was also performed for each 3s long segment of 8 Hz stimulus to find the SSVEP strength in each segment. Based on the network properties and SSVEPs calculated for each 3s-long segment of individual rat, the four properties of networks were correlated with the SSVEP strength for each rat to examine the possible dynamic relationships under each threshold (0.10 ∼ 0.28) (Figure 4(a) and Table 1).

4)8 Hz SSVEP strength versus network properties at the group level. The network properties and SSVEP strengths calculated for each segment were averaged to estimate the corresponding properties for individual rat under each threshold (0.10 ∼ 0.28), which are then used to estimate the correlation relationship between SSVEP strength and network properties across all rats in Figure 5(a) and Figure 6(a).

Similarly, to examine the relationship between the control state and 8 Hz SSVEP strength (Figure 5(b) and Figure 6(b)), for each rat, the corresponding network properties of those segments are further averaged to estimate the individual network properties for each rat under each threshold (0.10 ∼ 0.28) at the control state.

1. Regan, D. Human brain electrophysiology: Evoked potentials and evoked magnetic fields in science and medicine. (New York: Elsevier, 1989).
2. Herrmann, C. S. Human EEG responses to 1–100 Hz flicker: resonance phenomena in visual cortex and their potential correlation to cognitive phenomena. *Experimental brain research* **137**, 346–353 (2001).
3. Zhang, Y. *et al.* Multiple Frequencies Sequential Coding for SSVEP-Based Brain-Computer Interface. *PLoS One* **7**, e29519 (2012).
4. Wu, Z. & Yao, D. Frequency detection with stability coefficient for steady-state visual evoked potential (SSVEP)-based BCIs. *J Neural Eng* **5**, 36–43 (2008).
5. Ding, J., Sperling, G. & Srinivasan, R. Attentional modulation of SSVEP power depends on the network tagged by the flicker frequency. *Cereb Cortex* **16**, 1016–1029 (2006).
6. Mishra, J., Zinni, M., Bavelier, D. & Hillyard, S. A. Neural basis of superior performance of action videogame players in an attention-demanding task. *J Neurosci* **31**, 992–998 (2011).
7. Muller, M. M. *et al.* Feature-selective attention enhances color signals in early visual areas of the human brain. *Proc Natl Acad Sci U S A* **103**, 14250–14254 (2006).
8. Müller, M. M., Andersen, S. K. & Attar, C. H. Attentional Bias to Briefly Presented Emotional Distractors Follows a Slow Time Course in Visual Cortex. *The journal of neuroscience* **31**, 15914–15918 (2011).
9. Zhang, P., Jamison, K., Engel, S., He, B. & He, S. Binocular rivalry requires visual attention. *Neuron* **71**, 362–369 (2011).
10. Srinivasan, R. & Petrovic, S. MEG phase follows conscious perception during binocular rivalry induced by visual stream segregation. *Cerebral Cortex* **16**, 597–608 (2006).
11. Sutoyo, D. & Srinivasan, R. Nonlinear SSVEP responses are sensitive to the perceptual binding of visual hemifields during conventional 'eye' rivalry and interocular 'percept' rivalry. *Brain Res* **1251**, 245–255 (2009).
12. Wu, Z., Yao, D., Tang, Y., Huang, Y. & Su, S. Amplitude modulation of steady-state visual evoked potentials by event-related potentials in a working memory task. *Journal of biological physics* **36**, 261–271 (2010).
13. Wu, Z. & Yao, D. The influence of cognitive tasks on different frequencies steady-state visual evoked potentials. *Brain Topogr* **20**, 97–104 (2007).
14. Silberstein, R. B., Nunez, P. L., Pipingas, A., Harris, P. & Danieli, F. Steady state visually evoked potential (SSVEP) topography in a graded working memory task. *Int J Psychophysiol* **42**, 219–232 (2001).
15. Vialatte, F. B., Maurice, M., Dauwels, J. & Cichocki, A. Steady-state visually evoked potentials: focus on essential paradigms and future perspectives. *Progress in neurobiology* **90**, 418–438 (2010).
16. Di Russo, F. *et al.* Spatiotemporal analysis of the cortical sources of the steady-state visual evoked potential. *Hum Brain Mapp* **28**, 323–334 (2007).
17. Pastor, M. A., Artieda, J., Arbizu, J., Valencia, M. & Masdeu, J. C. Human cerebral activation during steady-state visual-evoked responses. *The journal of neuroscience* **23**, 11621 (2003).
18. Srinivasan, R., Fornari, E., Knyazeva, M., Meuli, R. & Maeder, P. fMRI responses in medial frontal cortex that depend on the temporal frequency of visual input. *Experimental brain research* **180**, 677–691 (2007).
19. Pastor, M., Valencia, M., Artieda, J., Alegre, M. & Masdeu, J. Topography of cortical activation differs for fundamental and harmonic frequencies of the steady-state visual-evoked responses. An EEG and PET H215O study. *Cerebral Cortex* **17**, 1899 (2007).
20. Srinivasan, R., Bibi, F. A. & Nunez, P. L. Steady-state visual evoked potentials: distributed local sources and wave-like dynamics are sensitive to flicker frequency. *Brain Topogr* **18**, 167–187 (2006).
21. Sammer, G. *et al.* Acquisition of typical EEG waveforms during fMRI: SSVEP, LRP, and frontal theta. *Neuroimage* **24**, 1012–1024 (2005).
22. Fawcett, I. P., Barnes, G. R., Hillebrand, A. & Singh, K. D. The temporal frequency tuning of human visual cortex investigated using synthetic aperture magnetometry. *Neuroimage* **21**, 1542–1553 (2004).
23. Yan, Z. & Gao, X. Functional connectivity analysis of steady-state visual evoked potentials. *Neuroscience letters* **499**, 199–203 (2011).
24. Liang, Z., King, J. & Zhang, N. Intrinsic organization of the anesthetized brain. *J Neurosci* **32**, 10183–10191 (2012).
25. Burkitt, G. R., Silberstein, R. B., Cadusch, P. J. & Wood, A. W. Steady-state visual evoked potentials and travelling waves. *Clin Neurophysiol* **111**, 246–258 (2000).
26. Paxinos, G. & Watson, C. The rat brain in stereotaxic coordinates. 5th edn, (Elsevier Academic Press, 2005).
27. Meeren, H. K., Pijn, J. P., Van Luijtelaar, E. L., Coenen, A. M. & Lopes da Silva, F. H. Cortical focus drives widespread corticothalamic networks during spontaneous absence seizures in rats. *J Neurosci* **22**, 1480–1495 (2002).
28. Meeren, H. K., Veening, J. G., Moderscheim, T. A., Coenen, A. M. & van Luijtelaar, G. Thalamic lesions in a genetic rat model of absence epilepsy: dissociation between spike-wave discharges and sleep spindles. *Exp Neurol* **217**, 25–37 (2009).
29. Rager, G. & Singer, W. The response of cat visual cortex to flicker stimuli of variable frequency. *European Journal of Neuroscience* **10**, 1856–1877 (1998).
30. Qin, Y., Xu, P. & Yao, D. A comparative study of different references for EEG default mode network: the use of the infinity reference. *Clin Neurophysiol* **121**, 1981–1991 (2010).
31. Koopmans, L. H. The spectral analysis of time series. (Academic Press, 1974).
32. Rubinov, M. & Sporns, O. Complex network measures of brain connectivity: uses and interpretations. *Neuroimage* **52**, 1059–1069 (2010).

Acknowledgements

This work was supported in part by grants from 973 program 2011CB707803, the National Nature Science Foundation of China (#61175117, #31070881 and #31100745, #91232725), the program for New Century Excellent Talents in University (#NCET-12-0089) and the 863 project 2012AA011601.

Author contributions

P.X., D.Y. conceived and designed the experiments. C.T., Z.W., W.J., X.Y. performed the experiment. P.X., C.T., Y.Z., Y.T., J.H., T.L. performed analysis for the dataset. P.X., C.T., Y.Z., D.Y. wrote the manuscript with input from all co-authors.

Additional information

Competing financial interests: The authors declare no competing financial interests.

How to cite this article: Xu, P. *et al*. Cortical network properties revealed by SSVEP in anesthetized rats. *Sci. Rep.* **3**, 2496; DOI:10.1038/srep02496 (2013).